earlier test configuration. In this case the inputs of the system were the initial state at entry interface and the angular rates flight history. (There is no thruster activity data from flight.) Thus, the system state at a given instant results from the state history since the beginning of simulation. This simulator configuration is more precise because the atmospheric model is in the loop. The test allows evaluation of the ARC models and validation of GESARED. Moreover, this test can also be used for postflight analysis, and the results obtained were compared with flight data. It can be concluded that there is an increase in error, mainly resulting from error propagation. Figure 1 shows the results of both tests, compared with the real flight data. Although errors are neglectable in the beginning of the simulation, they increase toward the end, being more significative for the second test configuration. The justification for this error lies in the aerodynamic database (both simulations) and in the error accumulation (second simulation). Because in the last part of the simulation the total velocity decreases, the relative importance of forces increase, making the discrepancies between real and predicted aerodynamics more visible. These results are considered satisfactory as GESARED six-DOF simulations using attitude as reference trajectory are shown to closely match real flight measurements.

Conclusions

A new reentry simulation tool, GESARED, was implemented in the MATLAB®/SIMULINK environment. The primary objective of this simulator is to be used as a design environment of GN&C systems for reentry vehicles. As a test bed, GESARED is also designed to facilitate performance evaluations against requirements in both nominal and off-nominal conditions, allowing the entire GN&C system development process to be condensed in one tool based on a compatible, versatile, and easy-to-use environment. Moreover, GESARED is also designed to make open-loop simulations possible for model verification or postflight analysis. GESARED, more than using the potentialities of the simulation environment, has itself an open structure, allowing extensibility and model modifications. The versatility is exemplified in the set of reentry vehicles (such as the LBRV or the ARC) that can be simulated using GESARED. In addition, other entry environments (such as Mars or Titan) can be simulated.

The validation of GESARED was performed by comparing simulation results with real flight data (for the ARC) and precomputed reentry trajectory (for the LBRV). The comparison between simulation results with the LBRV models in the loop and a reference trajectory allowed the validation of the three-DOF translational motion model, the atmospheric model, the Earth model, and the LBRV models. Comparison with ARC flight data allowed wider validation, in the sense that it was possible to compare this data with the aerodynamic model of the ARC, the environment models, and the six-DOF motion models. Thus, combining the three tests performed (two with the ARC model and another with the LBRV model) it was possible to fully validate GESARED and perform the ARC postflight analysis. From the second test with the ARC model in the loop, it can be concluded that there is a neglectable mismatch between the aerodynamic model and the real vehicle. The two ARC software validation tests gave insight on the importance of error accumulation in a process as reentry, characterized by large duration and significant variation of both environment and flight conditions. Flight controller design and postflight analysis for two representative reentry vehicles were successfully conducted using the simulation tool discussed in this paper. GESARED also shows potentials in GN&C design and analysis for different reentry vehicles and missions.

References

[1]Costa, R. R., Chu, Q. P., and Mulder, J. A., "Reentry Flight Controller Design Using Non-Linear Dynamic Inversion," *Proceedings of the Guidance, Navigation and Control Conference* [CD-ROM], AIAA, Reston, VA, 2001.

[2]Regan, F. J., and Anandakrishnan, S. M., *Dynamics of Atmospheric Re-Entry*, 1st ed., AIAA Education Series, AIAA, Washington DC, 1993, pp. 111–135.

[3]Mooij, E., *The Motion of a Vehicle in a Planetary Atmosphere*, 1st ed., Delft Univ. Press, Delft, The Netherlands, 1994, pp. 14–43.

[4]Wu, S. F., and Chu, Q. P., "The Atmospheric Re-Entry Spacecraft CRV/X-38—Aerodynamic Modeling and Analysis," ESA–European Space Technology Center, ESTEC Rept., Noordwijk, The Netherlands, July 2000.

[5]Wiegand, A., Markl, A., Well, K. H., Mehlem, K., Ortega, G., and Steinkopf, M., "AL-TOS—ESA's Trajectory Optimization Tool Applied to Re-Entry Vehicle Trajectory Design," *Proceedings of the 50th International Astronautical Federation Congress*, International Astronautical Federation, Amsterdam, 1999.

C. A. Kluever
Associate Editor

New Reliability Configuration for Large Planetary Descent Vehicles

Hüseyin Sarper* and Wolfang J. Sauer†
University of Southern Colorado, Pueblo, Colorado 81001

Introduction

THIS Note is based on presentations[1,2] at the past two conferences of the Mars Society. Several successive large vehicles must land in an attempt to establish the first human outpost. A single descent engine, as in the lunar module, is not under consideration because it would not provide enough reverse thrust to slow the vehicle and it would cause balance problems during landing. It was stated that, if one of the even number of engines fails while landing, the opposite engine would have to be shut off to maintain vehicle balance. The need to shut off the opposite engine presents a unique reliability problem, not readily found in the literature. Two new engine configurations are considered: a balanced four-engine (BFE) vehicle and a larger, balanced six-engine (BSE) vehicle. Figures 1 and 2 show these configurations, respectively. Both vehicles can land as long as each experiences at most one engine pair unavailability. (One engine fails, and the opposite engine is shut off.) The problem, at first, appears to be that of classic k-out-of-n (Ref. 3) reliability structure where any (random) k of the n ($k \leq n$) engines are sufficient, but this is not the case in the new problem. In fact, this problem has never been discussed in the literature before. These systems were proposed[1,2] as theoretical future powered vehicles, but they resemble Delta Clipper (or DC-X) vehicle. Visual inspection‡ shows four symmetrical thrust sources or engines. It appears that DC-X vehicle is relevant, and it should help to frame the state of the art. The purpose of this Note is not to perform reliability analysis of DC-X or another similar vehicle. The purpose is to provide reliability tools that can be used in making risk or probability statements on the performance of these new reliability structures, which can be used in determining the overall reliability of a large descent (or ascent) vehicle.

Problem Description and Solution

Discrete Random Variable Approach

Each engine's performance is actually a random variable. A discrete random variable is suitable if the consideration is whether an

Received 4 October 2001; revision received 8 April 2002; accepted for publication 8 April 2002.

*Professor of Engineering and Faculty Coordinator of Colorado Space Grant Consortium at USC, 2200 Bonforte Boulevard.

†Chair of Engineering Technology and Director of Colorado Space Grant Consortium at USC, 2200 Bonforte Boulevard.

‡Data available online at http://antwrp.gsfc.nasa.gov/apod/ap951028.html [cited 20 March 2002].

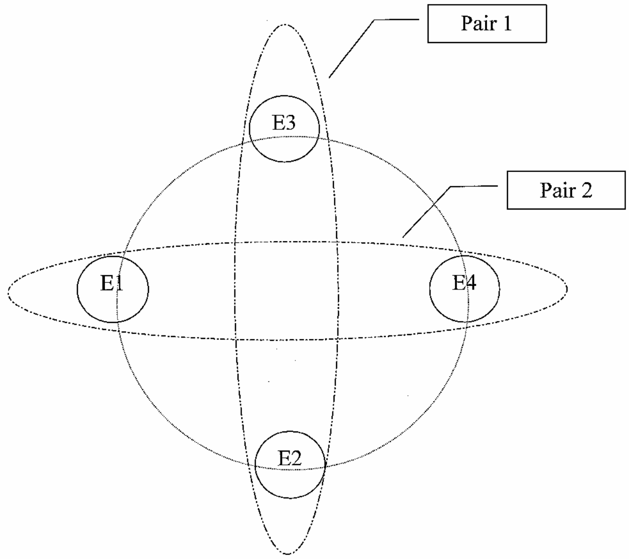

Fig. 1 Four-engine configuration (BFE).

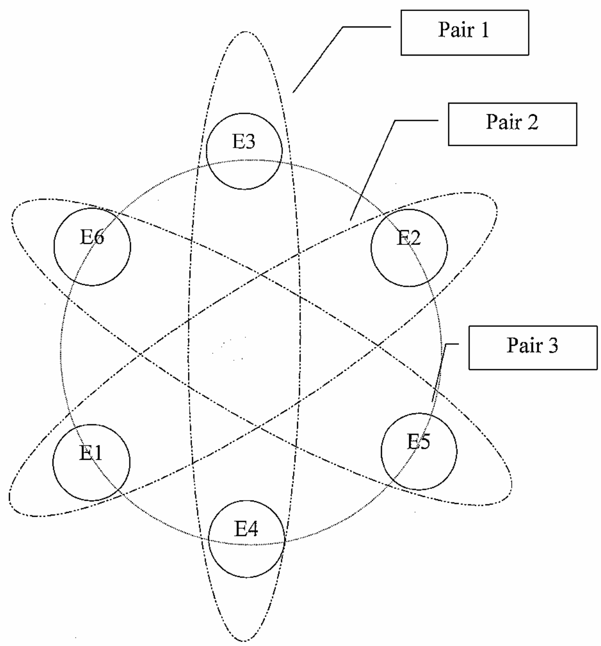

Fig. 2 Six-engine configuration (BSE).

engine will work (with a reliability or probability of p) or not for an implied time. The time can be thought of as the duration the vehicle takes to land after leaving the orbit. The random variable type governing the behavior of each engine is of Bernoulli kind.

Define X_i as follows:

$$X_i = \begin{cases} 1 & \text{if } i\text{th engine works until landing} \\ 0 & \text{otherwise} \end{cases}$$

BFE Case

Here, $P(X_i = 1) = p$ and $P(X_i = 0) = 1 - p$. X_i denotes the success (1) or failure (0) event for each engine. Let Z be the random variable associated with the successful landing of the vehicle and defined as follows:

$$Z = \begin{cases} 1 & \text{if rocket lands successfully} \\ 0 & \text{otherwise} \end{cases}$$

Let $X^{(i)}$ be the random variable denoting the success of the pair. Success of a pair is defined to be the success of each engine comprising the pair. Then, $P(X^{(i)} = 1) = p^2$ and $P(X^{(i)} = 0) = 1 - p^2$.

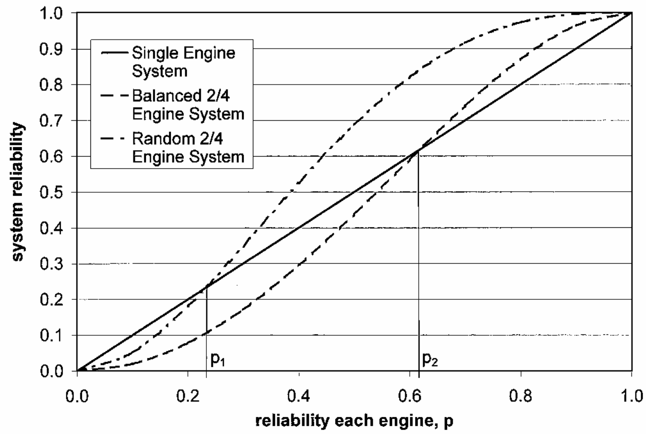

Fig. 3 Engine system: 2 out of 4.

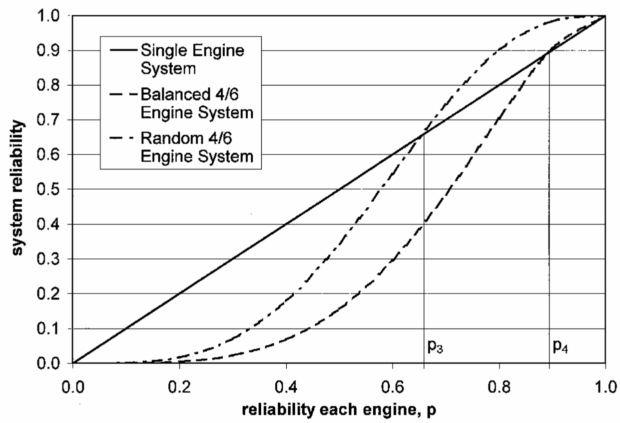

Fig. 4 Engine system: 4 out of 6.

For a successful landing, at least one pair must work until landing. The probability that none will work until landing is $P(X^{(1)} = 0) \times P(X^{(2)} = 0) = (1 - p^2)^2$, because X_i are independent. Then the probability of successful landing or the reliability expression is

$$P(Z = 1) = 1 - (1 - p^2)^2 \tag{1}$$

Figure 3 is a comparison of Eq. (1) with the reliability of the general (or random) 2-out-of-4 (Ref. 3) system (formula not shown) that may be applicable to a four-engine aircraft. The BFE case is less reliable than the general system for all p values, as one would expect, because this case has more restrictions than the general case where any two engines, not necessarily symmetric ones, can be out of service. The reliability of a single-engine vehicle plots as a straight line on both Figs. 3 and 4 and appears to provide higher reliability than the new balanced structures (BFE and BSE) and some of the general k-out-of-n structures for certain of the p values. This comparison is not practical because single engine is not a valid option, as discussed. With regard to the BFE case, a single engine is preferable (if it could provide enough reverse thrust and the balance problems were resolved) until the p value exceeds p_2, as shown in Fig. 3.

BSE Case

As in the BFE case, $P(X^{(i)} = 1) = p^2$ and $P(X^{(i)} = 0) = 1 - p^2$. For the BSE case, we need at least any two pairs out of three pairs working until landing. Then,

$$\begin{aligned} P(Z = 1) &= \binom{3}{2}[1 - (1 - p^2)]^2(1 - p^2) + [1 - (1 - p^2)]^3 \\ &= p^4(3 - 2p^2) \end{aligned} \tag{2}$$

Figure 4 shows a comparison of Eq. (2) with the reliability formula for the general (or random) 4-out-of-6 system.[3] The BSE case, again, is less reliable due to its additional physical restrictions. Figure 4 shows that the BSE system is better than a single engine (if this were a feasible option) if the engines are very reliable (p_4 or higher). Probability (and reliability) axioms are met in Figs. 3 and 4: All curves start and end at system values of 0 and 1. Perfect (and impossible) engines will result in a perfect (and impossible) system reliability of 1. Similarly, nonoperational engines (0 reliability) result in 0 system reliability, as expected. Figures 3 and 4 also show the classic tradeoff points (p_1 and p_3) between a single engine and the general (random) k-out-of-n systems.

Continuous Random Variable Approach

If time must be explicitly considered, then continuous random variables must be used. If the descent to the planet will take t minutes, then the minimum number of engine pairs must work at least that long for safe and successful landing. Define the following cumulative distribution functions (CDF):

$F_X(t)$ = CDF of each identical engine
$F_{X^{(i)}}(t)$ = probability that the ith pair will fail before time t
$F_Z(t)$ = probability that the mission (successful landing) will fail before time t

Derivations that follow are based on the extreme value distribution theory[4,5] of statistics. Extreme value-distribution-based procedures always use the CDF as the starting point in the mathematics.

BFE Case

Assume that there is only one pair; the pair will work until one of the engines fails. Let $X^{(1)}$ be the random variable associated with the time until failure of the first pair and X_i be the random variable associated with the time until failure of the ith engine, $X^{(1)} = \text{minimum}(X_1, X_2)$. The life of any pair is the shorter life of its two engines' lives. Hence,

$$
\begin{aligned}
P\left(X^{(1)} > t\right) &= P(X_1 > t, X_2 > t)\\
&= P(X_1 > t)P(X_2 > t)\\
&\qquad \text{(because engines are identical)}\\
&= [1 - F_X(t)]^2
\end{aligned}
$$

$$F_{X^{(1)}}(t) = 2F_X(t) - [F_X(t)]^2 \tag{3}$$

In the BFE case, there are two pairs, and at least one pair working properly is required for successful landing. The longer of the two pairs determines the duration of successful descent, $Z = \text{maximum}(X^{(1)}, X^{(2)})$. Thus, $P(Z \le t) = P(X^{(1)} \le t, X^{(2)} \le t)$, and because the engines and pairs are independent and identical,

$$
\begin{aligned}
P(Z \le t) &= P\left(X^{(1)} \le t\right)P\left(X^{(2)} \le t\right)\\
&= F_{X^{(1)}}(t)F_{X^{(2)}}(t)\\
&= [F_{X^{(1)}}(t)]^2\\
&= \left\{2F_X(t) - [F_X(t)]^2\right\}^2
\end{aligned}
$$

$$F_Z(t) = 4[F_X(t)]^2 - 4[F_X(t)]^3 + [F_X(t)]^4 \tag{4}$$

Equation (4) is a general CDF or failure function for the vehicle using any parent CDF that represents the life behavior of each engine. The reliability of the vehicle is the complement of Eq. (4).

BSE Case

Successful descent ends when the second engine pair fails (or as soon as any of two engines of that pair fails) because no more than one pair can be out of service in both BFE and BSE cases. Thus, $Z = \text{median}(X^{(1)}, X^{(2)}, X^{(3)})$. When steps similar to those given earlier are used, Eq. (5) is obtained. Equation (5) is a general CDF or failure function for the vehicle using any parent CDF that represents the life behavior of each engine:

$$
\begin{aligned}
F_Z(t) = {}& 3\left\{2F_X(t) - [F_X(t)]^2\right\}^2\left\{1 - 2F_X(t) + [F_X(t)]^2\right\}\\
&+ \left\{2F_X(t) - [F_X(t)]^2\right\}^3
\end{aligned} \tag{5}
$$

Table 1 Distribution parameters for system life

	BFE system		BSE system	
Parameter	Exponential	Uniform	Exponential	Uniform
Mean	$(3/4)\lambda^{-1}$	$(7/15)b$	$(5/12)\lambda^{-1}$	$(11/35)b$
Variance	$(5/16)\lambda^{-2}$	$(11/225)b^2$	$(13/144)\lambda^{-2}$	$(73/2450)b^2$
Median	$0.614\lambda^{-1}$	$0.458b$	$0.346\lambda^{-1}$	——[a]

[a]No closed-form solution is posssible; numerical solution is required.

Table 2 System reliability expressions

Case	Engine PDF	Reliability
BFE system	Exponential	$2e^{-2\lambda t} - e^{-4\lambda t}$
	Uniform	$1 - 4(t/b)^2 + 4(t/b)^3 - (t/b)^4$
BSE system	Exponential	$3e^{-4\lambda t} - 2e^{-6\lambda t}$
	Uniform	$1 - 12(t/b)^2 + 28(t/b)^3 - 27(t/b)^4 + 12(t/b)^5 - 2(t/b)^6$

Applications Using Two-Parent Engine Distribution Types

Exponential distribution or probability density function (PDF) is commonly used in reliability studies, and this distribution is sometimes a good representation of engineering phenomena as in the life of an engine. A nonnegative parameter λ is the inverse of the well-known mean time to failure or the mean value unique to this PDF [$f_x(t) = \lambda e^{-\lambda t}$] whose CDF is $F_X(t) = 1 - e^{-\lambda t}$, where t is also obviously nonnegative. Uniform PDF can also be used for illustration purposes. This PDF has a lower limit of 0 and an upper limit of b, where $b > 0$. The uniform PDF can be used to describe a situation when it is known that an engine cannot last longer than a known time value b. Unlike the exponential PDF, every life interval has equal probability using uniform PDF $(1/b)$ whose CDF is

$$
F_X(t) = \begin{cases} 0 & \text{if} \quad t < 0\\ t/b & \text{if} \quad 0 \le t \le b\\ 1 & \text{if} \quad t > b \end{cases} \tag{6}
$$

Equations (3) and (5) have been applied using these two-parent PDFs. Table 1 shows the parameters of the PDF that describe the duration of successful landing for both the BFE and BSE cases. Table 2 shows the reliability functions $R(t)$ for each case using both parent distributions. The failure function or the CDF $F(t)$, not shown, is $1 - R(t)$. The PDF expressions, also not shown (from which the parameters, except the median, shown in Table 1 are calculated), can be derived by differentiating the $F(t)$ function. The median expression is found by setting the $F(t)$ or $R(t)$ functions equal to 0.5.

Numerical Examples

Let us assume that the descent from a low Mars orbit takes $t = 6$ min and the engines have a mean life of 20 min. This corresponds to a λ value of $\frac{1}{20}$ for exponential and a b value of 40 [$(0 + b)/2 = 20$] for uniform engine life PDFs. The mean of 20 for each engine corresponds, using Table 1 formulas, to a mean life of 15 and 8.33 for BFE and BSE cases using exponential PDF. The mean lives are 18.67 and 12.57 for BFE and BSE using uniform pdf. Table 1 can be used to find the variance (and standard deviation) and the median of each case to have some idea about the risks about system life (safe and controlled descent time). For example, BFE vehicle's mean decent (available) time (life) is 15 min with a standard deviation of 11.18 min. The median available landing time

(life) of all such future vehicles will be experienced as 12.28 min using these engines. These results imply that 50% of all future landings will have descent times in excess of 12.28 min, but there is a real risk that there may not be enough time to cover the required minimum time of 6 required minutes in some landing attempts.

More precise risk information can be obtained using the reliability expressions. Application of the formulas in Table 2 results in a reliability of 0.7964 (BFE) and 0.5730 (BSE) using exponential PDF and 0.923 (BFE) and 0.8110 (BSE) using uniform PDF. These values are not very comforting, and the engines should be made stronger to last longer. A mean engine life of 30 min increases the reliabilities to 0.8913 (BFE) and 0.7436 (BSE) using exponential PDF and 0.9639 (BFE) and 0.9054 (BSE) using uniform PDFs. When the same order is used, a mean life of 60 min results in reliabilities of 0.9671, 0.9133, 0.9905, and 0.9733 for the same descent duration of 6 min. If 0.999 reliability is required, $R(t)$ expressions must be solved to find the parameters of the parent engine PDFs. The resulting mean values are as follows: 388.5 (BFE) and 666.7 (BSE) for exponential PDF and 188 (BFE) and 320 (BSE) for uniform PDF. This example illustrates the well-known diminishing returns in reliability calculations. Large improvements in each engine results in very small marginal gains in the overall system reliability. For example, the BSE system's engines (exponential case) would have to improve by a factor of 11 to increase system reliability by 9%.

Conclusions

This Note has addressed a new reliability configuration problem that may be needed in large future powered vehicle descent and possibly ascent design processes. Whereas Eqs. (3) and (5) are general for any parent PDF, it is not easy to derive closed-form reliability expressions for certain PDFs such as the normal and the general gamma distributions. Then, Monte Carlo simulation can be used in such cases. The specific formulas presented, however, can be used if exponential and uniform distributions are good representations for engine lives in a given problem. An analytical solution is always preferable over experimental (simulation) ones because the formulas are general for any given parameter. Another realistic extension should consider what happens to the life of the remaining engines as redundant pair fails. (Again, one engine of the pair fails and the opposite engine shut off.) The failure rates of the survivors must increase and simulation study may be appropriate. It is also assumed that all engines, within the pair and the entire vehicle, are independent of each other. This assumption may not always be true and the issue of dependency is a formidable mathematical challenge. This work would have to involve bivariate PDFs (instead of the univariate PDFs used in this Note) and/or correlation matrices to express statistical dependency among the engines within and across the engine pairs. The reader can refer to Johnson and Kotz[5] for an excellent discussion on multivariate (joint) PDFs with an emphasis on bivariate exponential PDF. Monte Carlo simulation will be necessary at some stage because analytical work quickly becomes highly intractable or impossible (even numerically) in dealing with dependent random variables found in engineering design problems.

References

[1]Brown, N., Hirata, C., and Shannon, R., "Mars Scheme: The Mars Society of Caltech Human Exploration of Mars Endeavor," *Third International Mars Society Convention*, Paper No. 5 in Track 2A, Aug. 2000.

[2]Brown, N., and Hirata, C., "The Mars Scheme IV: Trajectory Analysis," *Fourth International Mars Society Convention*, Paper No. 3 in Track 2D, Aug. 2001.

[3]Lewis, E. E., *Introduction to Reliability Engineering*, 2nd Ed., Wiley, New York, 1996.

[4]Sarper, H., "Extreme Value Flight Duration Analysis of Four Engine Spacecraft," *Journal of Spacecraft and Rockets*, Vol. 34, No. 3, 1997, pp. 402–405.

[5]Johnson, N. L., and Kotz, S., *Distributions in Statistics: Continuous Multivariate Distributions*, Wiley, New York, 1972, Chap. 4.

J. A. Martin
Associate Editor

Computational Investigation of Three-Dimensional Flow Effects on Micronozzles

R. D. D. Menzies,* B. E. Richards,† K. J. Badcock,‡
J. Löseken,§ and M. Kahl§
University of Glasgow,
Glasgow, Scotland G12 8QQ, United Kingdom

Introduction

SINCE the launch of Sputnik in 1957, there has been a steady growth in the size and weight of satellites. However, advances in miniaturization provide an opportunity to use smaller satellites. Microspacecraft development is technically demanding. Miniaturization is required in every subsystem including propulsion. Microelectromechanical systems (MEMS) is a new technology that can aid in the miniaturization of the propulsion system.

Deep reactive ion etching (DRIE) is one method among others of producing MEMS nozzles and is inherently two-dimensional. A material is placed on a two-dimensional silicon wafer, and a chemical reaction causes the nozzle pattern to be etched through to the wafer. Glass sheets are then anodically bonded to close the open channel. The silicon wafers used in recent experiments[1,2] were 308 μ thick, giving a nozzle depth H of 308 μ and a throat width typically of between 19 and 38 μ. A typical exit diameter is 100 μ, twice the size of a human hair.

Nearly all spacecraft nozzle shapes have been designed using inviscid flow theory. However, when dealing with such small devices the Reynolds numbers are low giving large boundary layers. The problem of low-Reynolds-number micronozzle flows has been examined at Massachusetts Institute of Technology (MIT),[1,2] where contoured converging-diverging nozzles were created and mass flow rates and thrusts measured. As the models had a large depth in comparison to the throat width, a two-dimensional model was used to predict viscous nozzle flow allowing comparison between experimental and computational measurements. It was found that experimentally measured mass flow rates matched well with predictions, whereas there was considerable discrepancy in thrust. This effect was presumed to be caused by the growth of the boundary layers on the upper and lower nozzle surfaces.

The aim of this work is to verify the findings for two-dimensional computations and experiment and then to investigate the extent of the three-dimensional effects. The computations have been done using the University of Glasgow's flow solver, Parallel Multi-Block (PMB).[3] Solutions were considered fully converged when the maximum residual had dropped eight orders of magnitude. Grid convergence was tested by running the calculations with double and half the number of grid points in each direction compared to a standard grid. Solutions were near identical for all grids used and were considered fully grid independent.

Received 20 February 2002; revision received 15 April 2002; accepted for publication 16 April 2002.

*Research Student, Department of Aerospace Engineering, Computational Fluid Dynamics Group; rmenzies@aero.gla.ac.uk.

†Mechan Professor, Department of Aerospace Engineering, Computational Fluid Dynamics Group. Associate Fellow AIAA.

‡Senior Lecturer, Department of Aerospace Engineering, Computational Fluid Dynamics Group.

§Undergraduate Student, Department of Aerospace Engineering, Computational Fluid Dynamics Group.